J of Nuclear Medicine Technology, first published online June 30, 2022 as doi:10.2967/jnmt.122.264058

Influence of minimum counts in brain perfusion SPECT: phantom and clinical studies.

Akie Sugiura[1,2], Masahisa Onoguchi[2], Takayuki Shibutani[2], and Yasuhisa Kouno[1]

[1] Department of Radiological Technology, Kariya Toyota General Hospital, 5-15 Sumiyoshi-cho, Kariya, 448-8505, Aichi, Japan

[2] Department of Quantum Medical Technology, Graduate School of Medical Sciences, Kanazawa University, 5-11-80, Kodatsuno, Kanazawa, Ishikawa, 920-0942, Japan

Corresponding Author: Masahisa Onoguchi, PhD

Department of Quantum Medical Technology, Graduate School of Medical Sciences, Kanazawa University, 5-11-80, Kodatsuno, Kanazawa, Ishikawa, 920-0942, Japan

Tel +81-76-265-2526, Fax +81-76-265-2526,

E-mail: onoguchi@staff.kanazawa-u.ac.jp

First Author: Akie Sugiura, MSc (in doctor's couse), RT.

Department of Radiological Technology, Kariya Toyota General Hospital, 5-15 Sumiyoshi-cho, Kariya, 448-8505, Aichi, Japan

Tel +81-566-21-2450, Fax +81-566-21-2450,

E-mail: sugiuraakie@gmail.com

Financial support: None

Short running title: Minimum counts in brain perfusion SPECT

Abstract

The counts per pixel of brain perfusion single photon emission computed tomography (SPECT) images depend on the administration dose, acquisition time or patient condition, and they sometimes become poor acquisition counts in daily clinical study. The aim of this study was to evaluate the effect of different acquisition counts on qualitative images and statistical imaging analysis and to determine the minimum acquisition counts necessary for accurate examinations. **Methods:** We performed a brain phantom experiment simulating normal accumulation of ^{99m}Tc -ethyl-cysteinate dimer (^{99m}Tc-ECD) as a brain uptake of 5.5 %. The SPECT data were acquired in a continuous repetitive rotation. Ten types of SPECT images with different acquisition counts were created by varying the addition of the number of rotations. We used the normalized mean squared error (NMSE) and visual analysis. For the clinical study, we used 25 patients acquired in a continuous repetitive rotation, and created six brain images with different acquisition counts by varying the number of rotations added from 1 to 6. The contrast-to-noise ratio (CNR) was calculated from the mean counts with regions of interest (ROIs) in gray and white matter. In addition, the severity, extent and ratio of disease-specific regions were evaluated as indices of statistical imaging analysis. **Results:** For the phantom study, the curve of NMSE showed a tendency of convergence from approximately 23.6 counts/pixel. Furthermore, the visual score showed that images with 23.6 counts/pixel or more were barely diagnosable. For the clinical study, the CNR was

significantly decreased at 11.5 counts/pixel or less. Severity and extent tended to increase with decreasing acquisition counts, and a significant increase was shown at 5.9 counts/pixel. On the other hand, there was no significant difference in ratio values among defferent acquisition counts.

Conclusion: Based on comprehensive assessment of phantom and clinical studies, we suggested that 23.6 counts/pixel or more were necessary to keep image quality of qualitative images and to accurately calculate indices of statistical imaging analysis.

Keywords

Brain perfusion imaging, Statistical imaging analysis, Artifact, Acquisition counts, Single photon emission computed tomography

Introduction

Brain perfusion single photon emission computed tomography (SPECT) has an important role in diagnosis of severity and prognosis of cerebral vascular disorders and identification of dementia, which contributes clinical management of patients (*1*). SPECT imaging has lower spatial resolution compared with morphological neuroimaging techniques such as computed tomography (CT) and magnetic resonance imaging (MRI), wheares allows for visualization and quantification of brain function and metabolism that are difficult to evaluate by other modalities.

In addition to visual interpretation of SPECT images, the statistical image analysis such as 3-dimensional stereotactic surface projections (*2*) and statistical parametric mapping (*3*) have been widely used, in which the individual brain image is transformed into a template and the relative regional uptake is compared voxel by voxel with the normal database to generate the Z-score of hypoperfusion (*4*). The results are projected onto the brain surface to create a surface representation of the Z-score (*5*), which facilitates the diagnosis of areas that are difficult to assess visually (*6*).

However, counts per pixel in brain perfusion SPECT image depends on administration dose, acquisition time or patient condition, and they sometimes become poor acquisition counts in daily clinical study. It is well known that statistical noise has a significant impact on image quality. The relationship between statistical noise (N) and counts per pixel (n) is expressed as $N = \sqrt{n}/n \times 100$ (*7*),

where signal-to-noise ratio of the SPECT image is proportional to square root of all counts, so as the number of acquisition counts decreases, statistical noise increases and image quality deteriorates.

The purpose of this study was to evaluate the effect of different acquisition counts on qualitative images and statistical imaging analysis and to determine the minimum acquisition counts necessary for accurate examinations. When clinical limitations result in low acquisition counts, we can pay attention to the interpretation of the qualitative images and the indices. Although published studies are available on the influence of acquisition and reconstruction methods (*8-10*), to our best knowledge, this is the first time that the minimum acquisition counts are addressed.

Materials and methods

Phantom design

A Hoffman 3D brain (Kyoto Kagaku, Co., Ltd., Kyoto, Japan) which simulates gray-matter and white-matter structures with 4:1 activity concentration was used as a phantom (*11*). The phantom is filled with a 37 kBq/mL solution of ^{99m}Tc. The total activity in the phantom was 44.4 MBq at acquisition start. It is assumed to be a normal accumulation of ^{99m}Tc-ethyl-cysteinate dimer (^{99m}Tc-ECD) with a

dose of 822 MBq as a brain uptake of 5.5 % (*12*). The dose was determined with reference to the subjects used in the clinical studies.

Patients

Images for 25 patients (16 men and 9 women; mean age, 75 ± 11.3 years), who underwent resting state brain perfusion ^{99m}Tc-ECD SPECT from March 2016 to March 2019, were retrospectively used in this study. These patients had degenerative nerve diseases (n = 22), cerebrovascular diseases (n = 3). The imaging diagnosis indicated decreased cerebral blood flow in all cases. Permission for this study was obtained from the hospital ethics committee.

Image acquisition

In both phantom and clinical studies, SPECT acquisition was performed with a dual-head gamma camera (Discovery NM/CT 670 Q.Suite pro, GE Healthcare Japan, Tokyo, Japan) equipped with a low-energy high-resolution collimator. The main energy window was 140.5 keV ± 10 % width. The sub-windows were set at 159.5 keV ± 3 % and 121.5 keV ± 4 % for scatter correction. The matrix size was 128 × 128, and the pixel size was 2.94 mm (1.5 zoom). The data were acquired in continuous mode of a 360-degree circular orbit (radius of rotation; 150 mm) and 90 projections of step angle 4 degrees.

For the phantom study, the acquisition time of SPECT was set as 3.5 min with 6 rotations, and subsequently 7.5 minutes with16 rotations (Fig. 1A).

For the clinical study, ^{99m}Tc -ECD (Fujifilm Toyam a Chemical, Co., Ltd., Tokyo, Japan) of 805 $\pm$ 40.1 MBq was injected intravenously, and 15 minutes later, images were acquired for 6 rotations at 3.5 minutes per projection (Fig. 1B).

Image reconstruction

The SPECT images were reconstructed using filtered back projection with a Ramachandran filter in the phantom and clinical studies. A Butterworth filter (order, 16; cutoff frequency, 0.55 cycles/cm) was utilized for the pre-filter for smoothing. The cut-off frequency of 0.55 cycles/cm was optimized in advance by caluculating the normalized mean squared error (NMSE) from high quality images with long acquisition time. The attenuation correction with the Chang method was performed assuming a uniform attenuation coefficient of 0.13 cm^{-1} and 10 % attenuation threshold. The triple-energy window method (*13*) was used for scatter correction. All images were reconstructed on a workstation using a Xeleris version.3.1 (GE Healthcare Japan, Tokyo, Japan).

Image evaluation

To measure the mean acquisition counts (counts/pixel), we drew a region of interest (ROI) surrounding whole brain on the anterior planar image of the projection data for phantom (Fig. 2A) (*14*). Brain images were created with 10 different acquisition counts (123.6, 92.3, 61.0, 30.8, 23.6, 19.9, 16.0, 12.0, 7.9 and 4.0 counts/pixel), respectively. The normalized mean squared error (NMSE) and visual analysis were used to assess each phantom image.

NMSE. The NMSE is given using the following equation:

$$NMSE = \frac{\sum_{x=0}^{x=n-1}\sum_{y=0}^{y=m-1}(f(x,y)-g(x,y))^2}{\sum_{x=0}^{x=n-1}\sum_{y=0}^{y=m-1}f(x,y)^2}$$

where f(x,y) is equal to the ideal image and g(x,y) is equal to the each phantom image. In this study, the ideal image was created by projections with high acquisition counts (123.6 counts/pixel) to redeuce the statistical noise. To assese precisely the convergence of the NMSE in relation to acquisition counts, we evaluated the derivative value of NMSE.

Visual analysis. We categorized 10 types of brain images based on how high the counts are into 5 scores with visual analysis. Five expert observers with expertise in nuclear medicine interpreted the transvers images (Fig. 3) To reduce variability in visual analysis, pre-training was carried out using sample images. At this time, we explained them to assume a clinical use not for scientific use and encouraged to observe cortical accumulation. They blindly assessed all series and scored each one (0-4). Details of the

scores are as follows: 4, very good; 3, sufficient for diagnosis; 2, barely diagnosable; 1, cannot be diagnosed responsibly; 0, cannot be diagnosed. The average score for all observers was calculated. The color lookup table was set to invert gray scale, and the upper and lower limits of the window level were set to 0 % and 100 %, respectevely. Furthermore, the enlargement and reduction of the images, observation distance, and observation time were arbitrary. We obtained written consent for all observers to participate in this study.

We created 6 brain images of different acquisition counts by patients, and they were obtained by varying the addition of the number of rotations on a workstation. The mean acquisition counts were measured setting a ROI on the normal or mild side on the anterior planar image of the projection data (Fig. 2B) (*14*). Patient images with a minimum of 30 counts/pixel were used to create. Based on the results of NMSE and visual analysis, we determined the image with 30 counts/pixel or more to be sufficient for diagnosis.

We used the contrast-to-noise ratio (CNR) and the indices from the program easy Z score imaging system (eZIS) (*4*) to assess the influence of low acquisition counts in qualitative images and statistical imaging analysis.

CNR. ROIs were automatically drawn on transverse image using the three-dimensional stereotaxic ROI template software, and average reconstructed image counts were calculated by dividing the brain into 12 segments (*15*). The CNR is given using the following equation:

$$CNR = (decreases\ of\ rCBF\ signal - background)/SD\ (background)$$

where decreases of regional cerebral blood flow (rCBF) signal is equal to the average reconstructed image counts in a ROI surrounding the areas diagnosed as decreases of rCBF on brain perfusion SPECT, background is the average reconstructed image counts of cerebellum ROIs, and standard division (SD) (background) is SD of cerebellum ROIs (*16*). Therefore, patients with decreases of rCBF in the cerebellum were excluded from the study. The CNR value was obtained from 6 brain images respectively and normalized by the value of the 6 rotations image.

eZIS analysis. The eZIS analysis is used to discriminate early Alzheimer's disease (AD) from other types of dementia using computer-assisted statistical analysis. The indices of eZIS that characterize rCBF decreases in patients with very early AD, namely, severity, extent, and ratio were calculated automatically analyzing the specific volume of interest (VOI) in the posterior cingulate gyrus, precuneus and parietal cortices. The severity and extent show the degree and percentage rate of rCBF decrease in the VOI. The ratio shows the percentage of rCBF decrease in the VOI to a whole brain. The severity,

extent and ratio were obtained from 6 brain images of different acquisition counts for each patient, respectively, and normalized by the values of the 6 rotations image. Patients with degenerative nerve diseases (n = 22) were analyzed because the eZIS was used in the differential diagnosis of dementia. We performed the eZIS analysis using a Daemon research image processor version. 1.1.0.0 (DRIP, Fujifilm Toyama Chemical Co., Ltd., Tokyo, Japan)

Statistical analysis

All statistical analyses were performed using the statistical package EZR (ver.1.38) (*17*). Visual scores were compared for differences using Kruskal Wallis/Steel's test. Wilcoxon signed-rank test with the Bonferroni correction was used to analyze CNR, severity, extent, and ratio among all image sets. *P* value of less than 0.01 was considered statistically significant.

Results

Phantom study

In the curve of NMSE in relation to acquisition counts, the tendency of convergence was observed with increasing acquisition counts (Fig. 4). The curve of the derivative value of NMSE showed

a rapid increase at low acquisition counts, followed by saturation as close to zero as possible above 23.6 counts/pixel (Fig. 5).

The visual score increased with increasing acquisition counts. And it showed enough higher score than “2, barely diagnosable” at 23.6 counts/pixel or more, and enough higher score than “3, sufficient for diagnosis” at 30 counts/pixel or more (Fig. 6).

Clinical study

The CNR was significantly decreased at 11.5 counts/pixel or less (p<0.01, Table. 1).

Severity and extent tended to increase with decreasing acquisiton counts, and a significant increase was shown at 5.9 counts/pixel (p<0.01). On the other hand, ratio was independent of acquisiton counts and there was no significant difference in ratio values among acquisition counts. (Table 2). Difference of the average counts per pixel between Tables 1 and 2 was caused by that of numbers of patients analyzed in CNR and eZIS analysis. Figure 7 shows a comparison of the 6 rotations image (32.9 counts/pixel) with the image obtained at low acquisition counts (6.2 counts/pixel) using statistical imaging analysis.

Discussion

Recent dementia practice guidelines recommend the use of morphological imaging (MRI or CT) for excluding neurosurgical dementia and then functional imaging (brain perfusion SPECT or dopamine transporter scintigraphy) for making a differential diagnosis (*18*). Brain perfusion SPECT is commonly used in differential diagnosis of dementia by assessing pattern of hypoperfusion for each type of dementia, and it is also expected to be used for early diagnosis of AD in patients with mild cognitive impairment (MCI) (*19*). On the other hand, in daily practice for patients with dementia, the characteristic symptoms of the patients may force to interrupt or shorten the scan. A consequence is that they sometimes lead poor acquisition counts. Therefore, it is important to reveal the effect of different acquisition counts and the minimum acquisition counts necessary for accurate examinations. We believed that this study was useful for daily clinical study.

Many researches previously have been dealt with the image quality improvement in brain perfusion SPECT by reducing image noise. As a result, it is now possible to obtain images with less statistical noise by optimizing the low-pass filter or using multi-pinhole collimators (*8*,*9*). Furthermore, it has been reported that the iterative reconstruction technology with resolution recovery algorithm is

possible to improve spatial resolution while suppressing statistical noise (*10*). However, studies on decreases of acquisition counts are insufficient, although they may occur in daily clinical study.

As a result of the phantom study, we considered 23.6 counts/pixel or more necessary to keep image quality because the NMSE showed a convergence at 23.6 counts/pixel or more, and the score with visual analysis was enough higher than "2, barely diagnosable" at 23.6 counts/pixel or more. NMSE is commonly used in order to optimize the low pass filter or the iteration number, and well reflects the influence of statistical noise on SPECT images (*8,10*). Furthermore, it is assumed that statistical noise did not affect on the ideal image of the NMSE because we reconstructed the ideal image from projection data with statistical noise lower than 10% applying optimized Butterworth filter. In addition, visual assessment by scoring is also used in nuclear medicine imaging widely (*20*). Therefore, the obtained results are reliable.

In the clinical study, the value of CNR showed a significant decrease at 11.5 counts/pixel, and we decided that 17.2 counts/pixel or more did not affect the detection of decreases in rCBF. The values of severity and extent tended to increase with the decreasing acquisition counts, and a significant increase was shown at 5.9 counts/pixel ($p<0.01$). It is assumed that statistical noise was determined as a hypoperfusion area in the specific VOI during eZIS analysis (*21*), and we need to take note of false positive in differential diagnosis of dementia using eZIS analysis. We decided that 11.6 counts/pixel or

more did not affect the values of severity and extent. The reason why the minimum acquisition counts of severiry and extent are lower than that of CNR is because of smoothing process included in eZIS analysis process (*22*). On the other hand, the value of ratio was independent of the acquisition counts. This suggests that the influence of statistical noise was not only on the specific VOI but also on the whole brain. The phantom study simulated normal human brain, whereas the clinical study addressed detection of cerebral hypoperfusion. Therefore, we considered that difference between visual analysis of phantom study and the results of clinical investigation occured.

Based on comprehensive assessment of phantom and clinical studies, we determined that 23.6 counts/pixel were the minimum acquisition counts to keep image quality of qualitative images and to accurately calculate indices of statistical imaging analysis. Generally, more than 100 counts/pixel were needed to suppress statistical noise (*7*). Stelter et al. (*23*) also suggested 50 counts/pixel or more for sufficient image quality. We considered that our result differed from previous studies because this research dealt with the minimum acquisition counts, not with sufficient image quality. The presence of cerebral ventricles in the ROI we set may also effect the acquisition counts. For routine brain perfusion SPECT examinations, we recommend using the proposed minimum acquisition counts as the criterion for re-examination or a warning to the physician.

There are some limitations of this study. Firstly, we categorized 10 types of brain images to five scales of image quality by visual analysis, but five scales of image quality are actually vague and may include various aspects of image quality such as observer preference. Therefore, when setting the cut-off for the counts, we selected 30.0 counts/pixel or 23.6 counts/pixel at which the score was enough higher than 3 or 2 in order to have margins. Further study should be conducted to clarify the differences of five scales and to reveal the relationship between sub-ideal image quality and diagnostic accuracy. Second limitation is difference between devices. Differences in reconstruction methods, low pass filters, or various correction methods are surmised to affect the minimum acquisition counts. But we considered that the results of statistical imaging analysis are widely applicable to other devices because it reduces the differences between devices by anatomical standardization and smoothing process. The minimum acquisition counts can lead to precise diagnosis and shorter scan times. Furthermore, in young patients, it is expected to reduce exposure of radiation by optimizing dosage of radiopharmaceuticals. Therefore, in the future, it is desirable to determine the minimum acquisition counts considering difference between devices.

Conclusion

Based on comprehensive assessment of phantom and clinical studies, we suggested that 23.6 counts/pixel or more were necessary to keep image quality of qualitative images and to accurately

calculate indices of statistical imaging analysis. The proposed minimum acquisiton counts will help raise reliability of brain perfusion SPECT, for example, by means of the criterion for re-examination or a warning to the physician.

Disclosure

No potential conflict of interest relevant to this article was reported.

Acknowledgments

The authors thank the staff at the Department of Radiological Technology, Kariya Toyota General Hospital for providing technical support.

Key Points

Question: How is the minimum acquisiton counts for brain perfusion SPECT?

Pertinent findings: phantom and clinical study, 23.6 counts/pixel

Implications for patient care: The proposed minimum acquisiton counts will help raise reliability of brain perfusion SPECT

References

1. Camargo EE. Brain SPECT in neurology and psychiatry. *J Nucl Med*. 2001;42:611-623.

2. Minoshima S, Frey KA, Koeppe RA, Foster NL, Kuhl DE. A diagnostic approach in Alzheimer's disease using three-dimensional stereotactic surface projections of fluorine-18-FDG PET. *J Nucl Med*. 1995;36:1238–48.

3. Friston KJ, Frith CD, Fletcher P, Liddle PF, Frackowiak RS. Functional topography: multidimensional scaling and functional connectivity in the brain. *Cereb Cortex*. 1996;6:156–64.

4. Kanetaka H, Matsuda H, Asada T, et al. Effects of partial volume correctionon discrimination between very early Alzheimer's dementia and controls using brain perfusion SPECT. *Eur J Nucl Med Mol Imaging.* 2004;31:975–80.

5. Matsuda H, Mizumura S, Nagao T, et al. Automated discrimination between very early Alzheimer disease and controls using an easy *Z* score imaging system for multicenter brain perfusion single-photon emission tomography. *Am J Neuroradiol*. 2007;28:731–6.

6. Imabayashi E, Matsuda H, Asada T, et al. Superiority of 3-dimensional stereotactic surface projection analysis over visual inspection in discrimination of patients with very early Alzheimer's disease from controls using brain perfusion SPECT. *J Nucl Med*. 2004;45:1450-7.

7. AE Todd-Pokropek, PH Jarritt. The noise characteristics of SPECT systems. *Computed Emission*

Tomography. 1982;361-89.

8. Minoshima S, Maruno H, Yui N, et al. Optimization of Butterworth filter for brain SPECT imaging. *Ann Nucl Med.* 1993;7:71-77.

9. Chen L, Tsui BM, Mok GS. Design and evaluation of two multi-pinhole collimators for brain SPECT. *Ann Nucl Med.* 2017;31:636-648.

10. Yokei T, Shinohara H, Onishi H. Performance evaluation of OSEM reconstruction algorithm incorporating three-dimensional distance-dependent resolution compensation for brain SPECT: A simulation study. *Ann Nucl Med*. 2002;16:11-18.

11. Hoffman EJ, Cutler PD, Diby WM, Mazziotta JC. Three dimensional phantom to simulate cerebral blood flow and metabolic images for PET. *IEEE Trans Nucl Sci.* 1990;37:616–20.

12. Kubo A, Nakamura K, Tsukatani Y, et al. Phase I clinical study of 99mTc-ECD. *Kaku igaku*, 1992; 29:1019-27.

13. Ogawa K, Harata Y, Ichihara T, Kubo A, Hashimoto S. A practical method for position-dependent Compton-scattered correction in single photon emission CT. *IEEE Trans Med Imaging.* 1991;10:408-12.

14. Yamanaga T, Hasegawa S, Imoto A, et al. Guidelines for standardization of brain perfusion SPECT imaging 1.0. *Kakuigakugijutsu*. 2017;37:505–16 (in Japanese).

15. Takeuchi R, Yonekura Y, Matsuda H, Konshi J: Usefulness of a three-dimensional stereotaxic ROI template on anatomically standardised 99m Tc-ECD SPET. *Eur J Nucl Med Mol Imaging*. 2002;29:331-41.

16. Matsuda H, Mizumura S, Nagao T, et al. An easy Z-score imaging system for discrimination between very early Alzheimer's disease and controls using brain perfusion SPECT in a multicentre study. *Nucl Med Commun*. 2007;28:199-205.

17. Kanda Y. Investigation of the freely available easy-to-use software 'EZR'for medical statistics. *Bone marrow transplantation.* 2013;48:452-458.

18. Ngo J, Holroyd-Leduc JM. Systematic review of recent dementia practice guidelines. *Age Ageing*. 2015;44:25-33.

19. Ito K, Mori E, Fukuyama H, et al. Prediction of outcomes in MCI with 123 I-IMP-CBF SPECT: a multicenter prospective cohort study. *Ann Nucl Med.* 2013;27:898-906.

20. Fukukita H, Suzuki K, Matsumoto K, et al. Japanese guideline for the oncology FDG-PET/CT data acquisition protocol: synopsis of Version 2.0. *Ann Nucl Med*. 2014;28:693-705.

21. Yanamoto T, Onishi H, Murakami T, Takahashi M, Odajima S, Uchida K. Research report: accuracy and evaluation of the stereotactic statistical imaging analysis of the brain. *Nippon Hoshasen Gijutsu Gakkai Zashi*. 2008;64:752–65 (in Japanese).

22. Yamamoto Y, Onoguchi M. Statistical image analysis method to use for cerebral blood flow SPECT examination: difference and matters that require attention of processing of eZIS and iSSP. *Nihon Hoshasen Gijutsu Gakkai Zasshi*. 2011;67:718–727 (in Japanese).

23. Stelter P, Junik R, Krzyminiewski R, Gembicki M, Sowin'ski J. Semiquantitative analysis of SPECT images using 99Tc(m)-HMPAO in the treatment of brain perfusion after the attenuation correction by the Chang method and the application of the Butterworth filter. *Nucl Med Commun*. 2001;22:857-65.

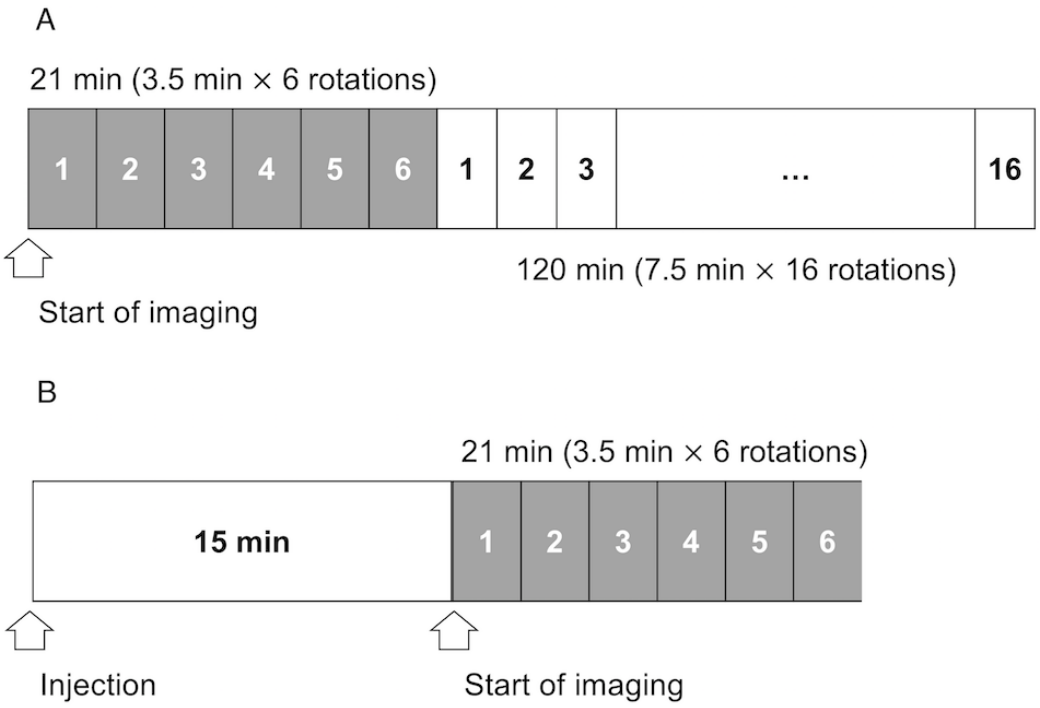

Figure 1. Protocols of SPECT data acquisition in this study.

A) Phantom study protocol. Images are acquired for 3.5 minutes with 6 rotations and subsequently 7.5 minutes with 16 rotations.

B) A brain perfusion SPECT protocol using ^{99m}Tc-ECD in clinical study. Images are acquired for 21 minutes [(3.5 min / rotation) × 6 rotations], beginning 15 minutes after the injection.

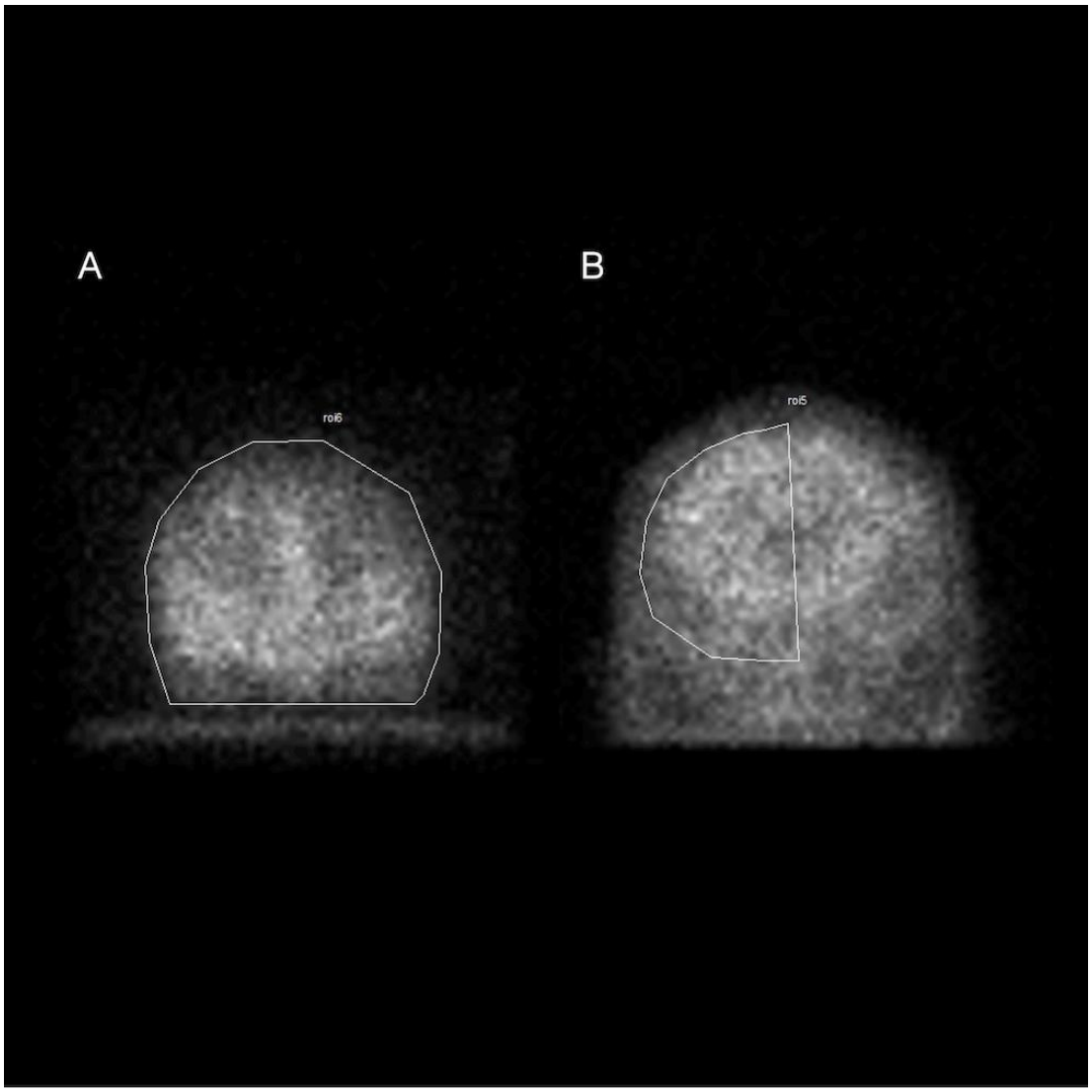

Figure 2. The illustration of brain image setting ROI. A ROI of the phantom study sets to surround a whole brain on the anterior planar image of the projection data (A). A ROI of the clinical study sets to surround a normal or mild side on the anterior planar image of the projection data (B).

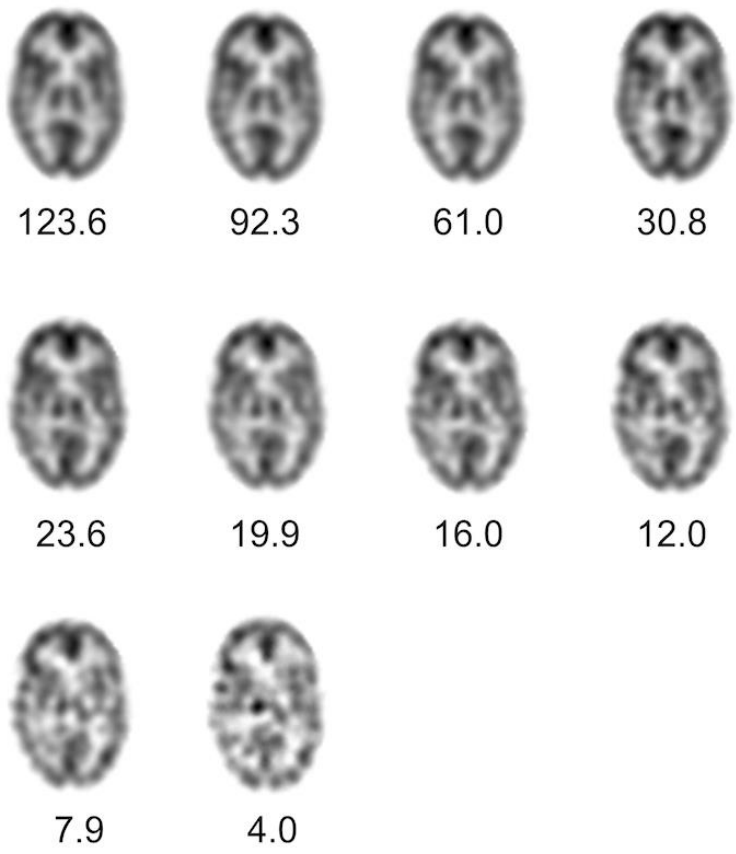

Figure 3. Representative slices of images for visual analysis. Images were created from ten types of projection data with different acquisition counts (123.6, 92.3, 61.0, 30.8, 23.6, 19.9, 16.0, 12.0, 7.9 and 4.0 counts/pixel).

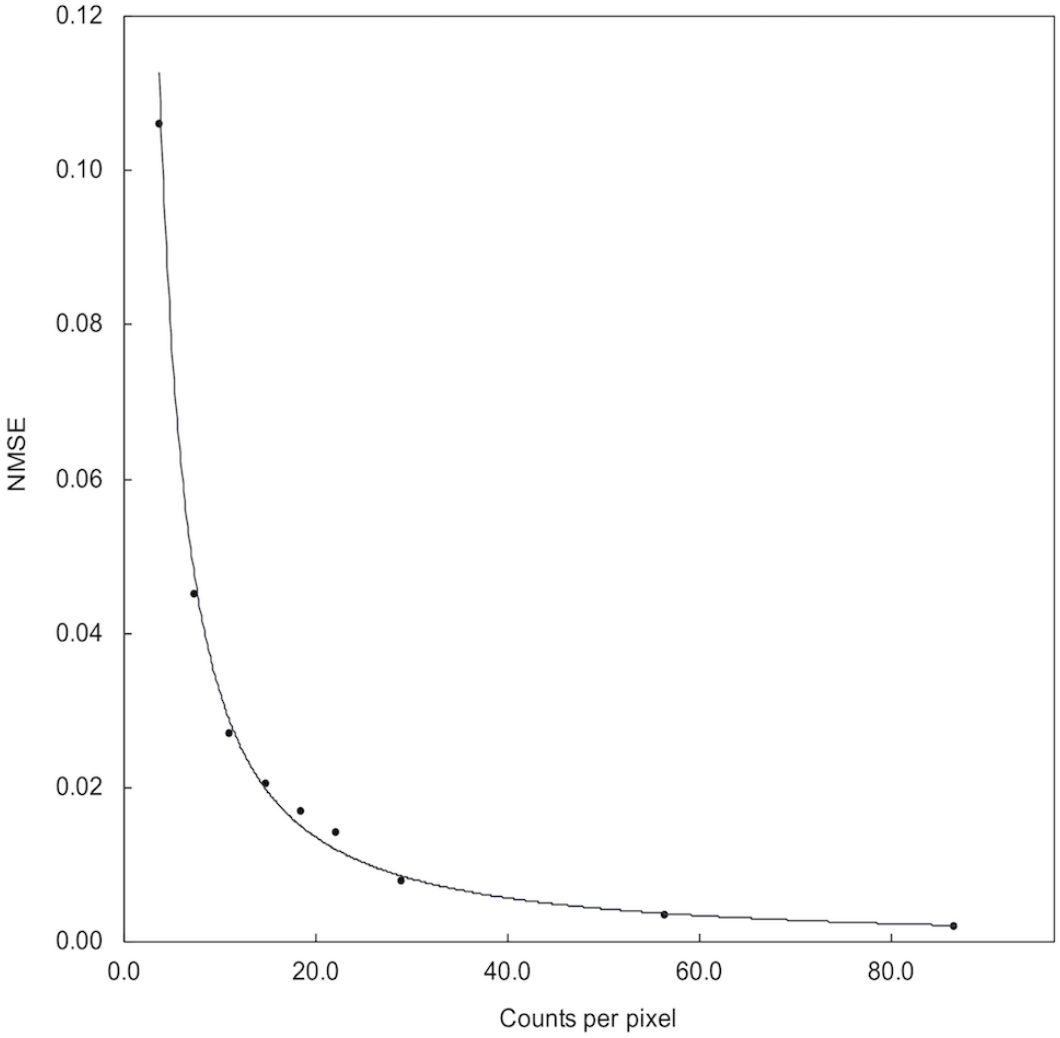

Figure 4. The NMSE as function of counts per pixel in the brain phantom.

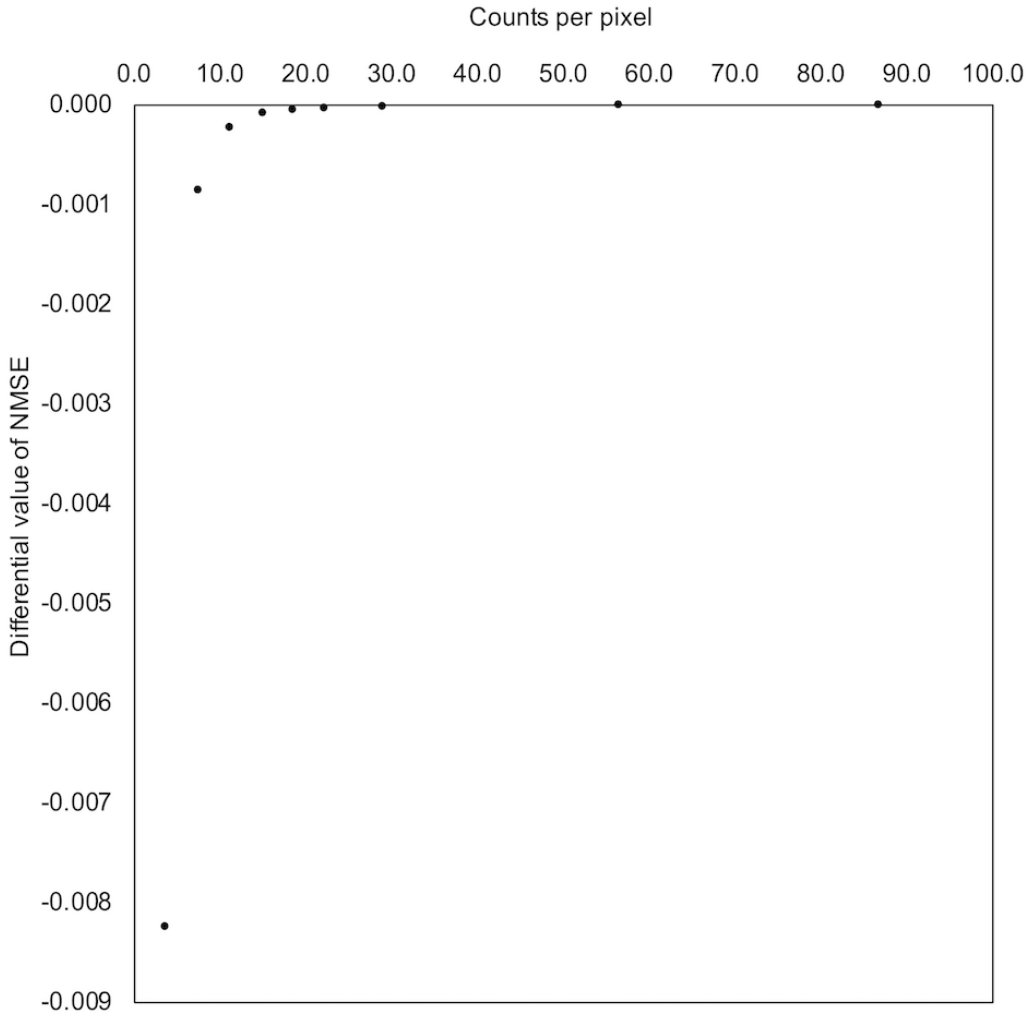

Figure 5. The differential value of NMSE as function of counts per pixel.

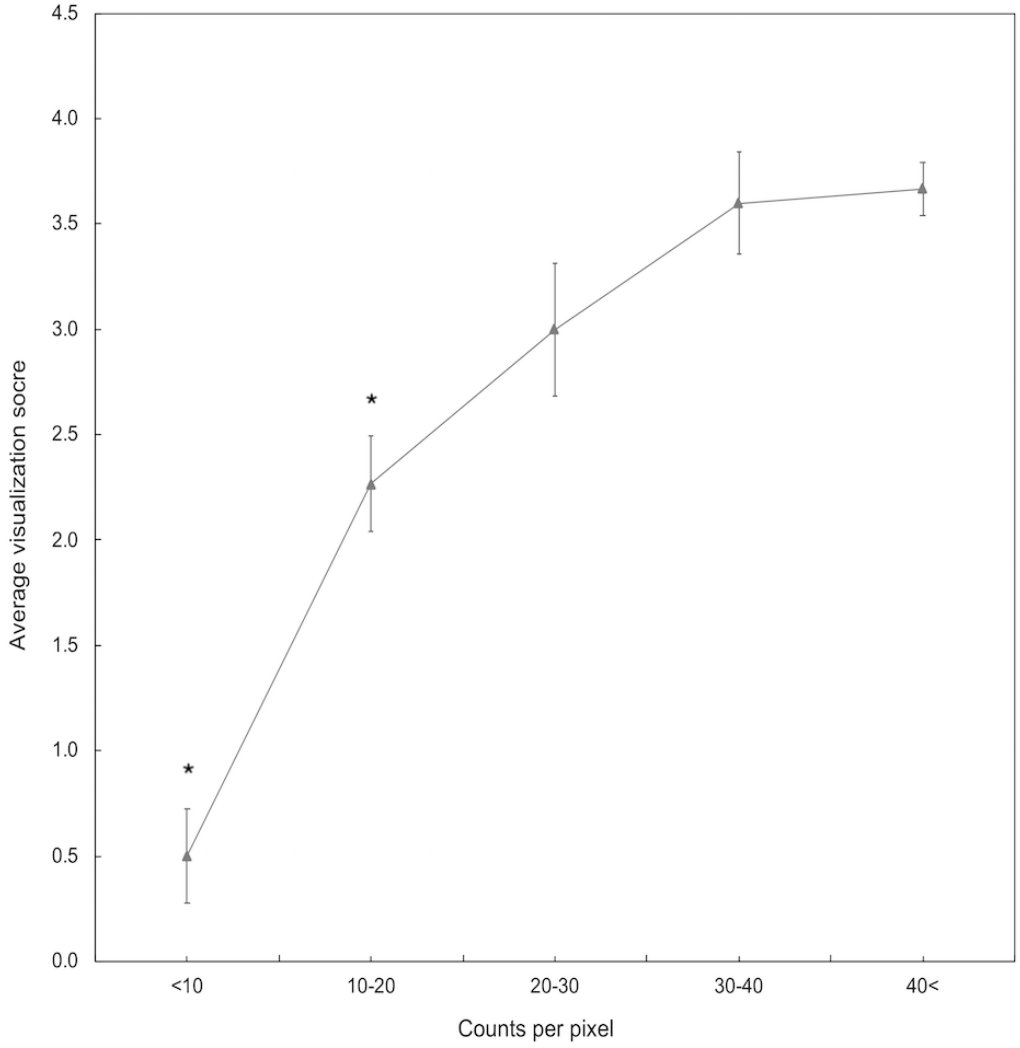

Figure 6. Relationship between average visualization score and each of the counts per pixel. * : vs 40 counts per pixel or more, $p<0.01$.

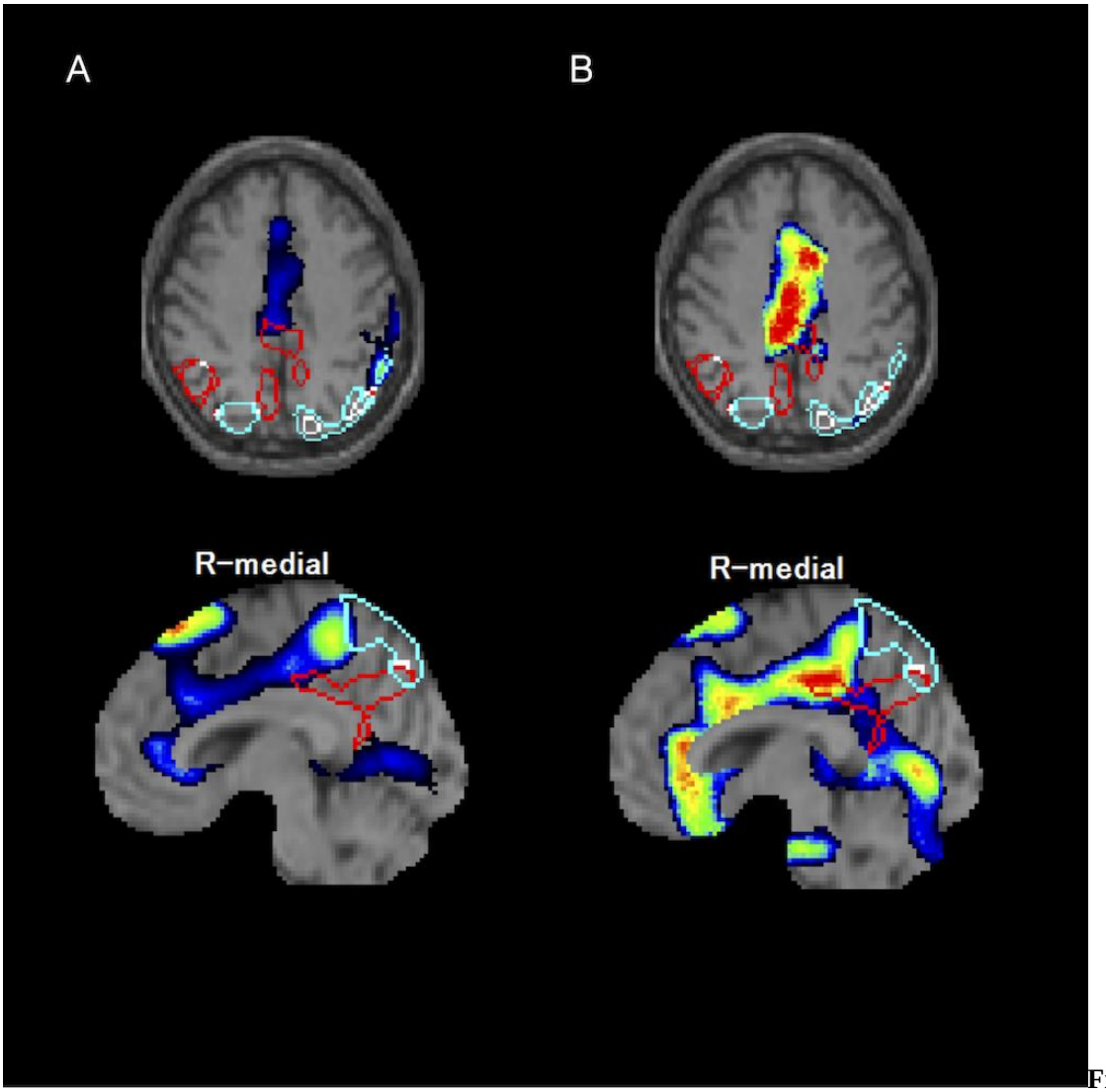

Figure 7. Typical brain perfusion images using the statistical image analysis obtained at different counts in a patient. Refference image (A). The image obtained at 32.9 (A), 6.2 (B) counts per pixel. False positives were observed in the specific VOI (red border).

Table 1. The average and SD of the CNR at different counts per pixel.

	6 rotation	5 rotation	4 rotation	3 rotation	2 rotation	1 rotation
counts/pixel	33.6 (±4.25)	28.3 (±3.55)	22.7 (±2.86)	17.2 (±2.17)	11.5 (±1.45)	5.9 (±0.73)
normalized CNR	1.00 (±0.0)	0.99 (±0.08)	0.96 (±0.10)	0.92 (±0.16)	0.84 (±0.17) *	0.56 (±0.25) *

Patients with degenerative nerve diseases (n = 22) and cerebrovascular diseases (n = 3) were analyzed.
* : vs 33.6 counts per pixel, p<0.01.

Table 2. The average and SD of the indices (severity, extent and ratio) at different counts per pixel.

	6 rotation	5 rotation	4 rotation	3 rotation	2 rotation	1 rotation
counts/pixel	33.9 (±4.45)	28.5 (±3.72)	22.9 (±2.99)	17.3 (±2.28)	11.6 (±1.52)	5.9 (±0.77)
normalized severity	1.00 (±0.0)	1.01 (±0.05)	1.05 (±0.06)	1.05 (±0.08)	1.07 (±0.15)	1.50 (±0.47) †
normalized extent	1.00 (±0.0)	1.00 (±0.12)	1.11 (±0.15)	1.18 (±0.55)	1.11 (±0.41)	2.34 (±2.12) †
normalized ratio	1.00 (±0.0)	0.97 (±0.11)	1.02 (±0.14)	1.01 (±0.51)	0.84 (±0.28)	1.33 (±1.17)

Patients with degenerative nerve diseases (n = 22) were analyzed. † : vs 33.9 counts/pixel, p<0.01.

Graphical Abstract